



## Injectable *in situ* forming nanogel: A hybrid Alginate-NLC formulation extends bupivacaine anesthetic effect

Gustavo H. Rodrigues da Silva<sup>a</sup>, Gabriela Geronimo<sup>a</sup>, Lígia N.M. Ribeiro<sup>a</sup>, Viviane A. Guilherme<sup>a</sup>, Ludmilla David de Moura<sup>a</sup>, André L. Bombeiro<sup>c</sup>, Juliana Damasceno Oliveira<sup>a</sup>, Márcia C. Breitzkreitz<sup>b</sup>, Eneida de Paula<sup>a,\*</sup>

<sup>a</sup> Department of Biochemistry and Tissue Biology, Institute of Biology, University of Campinas – UNICAMP, Campinas, São Paulo, Brazil

<sup>b</sup> Department of Analytical Chemistry, Institute of Chemistry, UNICAMP, Campinas, São Paulo, Brazil

<sup>c</sup> Department of Structural and Functional Biology, Institute of Biology, University of Campinas – UNICAMP, Campinas, São Paulo, Brazil

### ARTICLE INFO

#### Keywords:

Hybrid formulation  
Biopolymers  
Alginate  
Lipid nanoparticles  
Drug delivery  
Bupivacaine

### ABSTRACT

Finding an ideal anesthetic agent for postoperative pain control, with long action and low side effects, is still a challenge. Local anesthetics have potential for such application if their time of action is improved. This work introduces a new hybrid formulation formed by the association of a nanostructured lipid carrier with a biopolymeric system to encapsulate bupivacaine (BVC). The hybrid formulation was physicochemical and structurally characterized by DLS, TEM, DSC, XRD and FTIR-ATR, and it remained stable for 12 months at room temperature. *In vivo* analgesia and imaging tests showed that the hybrid system was able to modulate the release, and to increase the concentration of BVC at the site of action, by forming a nanogel *in situ*. Such nanogel improved over 5 times (> 24 h) the anesthesia duration, when compared to free BVC at clinical (0.5%) doses. Therefore, this novel *in situ*-forming nanogel shows great potential to be used in postsurgical pain control, improving the action of BVC, without losing its versatility of (infiltrative) application.

### 1. Introduction

Pain control, especially in the postoperative period, lacks advances in terms of ideal agents - with low adverse effects and fast patients recovery, so that to decrease medical expenses/length of hospital stay [1]. Local anesthetics (LA) are extensively used for surgical pain control, with well-defined protocols. However, due to their (CNS and CVS) systemic toxicity, and relatively short half-times (hours), LA become useless to produce analgesia for prolonged periods such as in postoperative period [2]. The development of Drug Delivery Systems (DDS), that keep the local anesthetic in the site of application and retard their systemic metabolization could increase the analgesia duration with no adverse systemic effects. In this way LA-in-DDS could replace the use of opioids - which have several side effects - in the postoperative pain control [3].

Nanostructured lipid carriers (NLC) are nanometric lipid-based carriers that show many advantages, such as increased upload capacity, improving the therapeutic activity of drugs by retarding their systemic degradation and providing sustained drug release [4]. NLC benefits

include safety - due to the use of biocompatible and functional excipients with reduced cytotoxicity, stability and low cost, making them attractive for the pharmaceutical and cosmetic industries [5–8]. The biopolymer alginate is a polysaccharide widely used in DDS because of its biocompatibility and easy to obtaining. In the presence of bivalent cations, such as  $\text{Ca}^{2+}$ , alginate gets ionically crosslinked in an “eggbox complex” [9,10]. These changes in alginate molecular structure result in a gel of decreased solubility [11].

Biohybrid systems describe the association between two DDS (one polymeric and another from organic material, e.g. lipids), which separated, might not bring about the maximum pharmaceutical performance of a chosen drug [12], as their association does. NLC are excellent carriers for local anesthetics, being able to prolong the anesthesia time as reported for different agents, and mainly for topical administration [2,13–15]. Alginate, by the other hand, allows the production of a liquid, injectable formulation (versatile for a local anesthetic) that after *in situ* gelation [16,17] is able to keep the NLC at the application site [18]. So, the association between these two carriers could bring advantages for the therapeutic use of local anesthetics.

\* Corresponding author at: Department of Biochemistry and Tissue Biology, Institute of Biology, University of Campinas - UNICAMP, Rua Monteiro Lobato, 255, Cid. Universitária Zeferino Vaz, Campinas, São Paulo 13083862, Brazil.

E-mail address: [depaula@unicamp.br](mailto:depaula@unicamp.br) (E. de Paula).

<https://doi.org/10.1016/j.msec.2019.110608>

Received 6 August 2019; Received in revised form 20 December 2019; Accepted 26 December 2019

Available online 28 December 2019

0928-4931/ © 2019 Elsevier B.V. All rights reserved.

BVC is the anesthetic of choice for surgical procedures, and its enantiomeric excess preparation (S75:R25, Novabupi®) has been successfully encapsulated into NLC [13,19]. Thus, the present work aimed at developing a hybrid formulation composed of NLC, alginate and 0.5% enantiomeric excess bupivacaine. The obtained hybrid formulation was characterized using dynamic light scattering (DLS), transmission electron microscopy (TEM), differential scanning calorimetry (DSC), powder X-ray diffraction (XRD) and infrared spectroscopy (FTIR-ATR) and its physical chemical stability was accompanied over 12 months at ambient temperature. Then, *in vitro* release kinetics, *in vivo* analgesic effect and NLC tracking imaging evidenced the sustained release and efficiency of the developed DDS.

## 2. Materials and methods

### 2.1. Materials

Bupivacaine S75:R25 hydrochloride (BVC) was donated by Cristália Prod. Quim. Farm. Ltda. (Brazil). Cetyl palmitate (CP) was purchased from Dhaymers Química Fina (Brazil) and Capryol 90® was donated by Gattefossé (France). The surfactant Pluronic® F68 (P68) and alginic acid sodium salt from brown algae (medium viscosity; MW 216 g/mol) (ALG) were supplied by Sigma (USA). The fluorescent dye DID (1,1'-diocadecyl-3,3',3',3'-tetramethylindodicarbocyanine perchlorate) was supplied by Invitrogen Corp (Eugene, OR). Deionized water (18 MΩ) was obtained from an Elga USF Maxima ultra-pure water purifier.

### 2.2. Formulation preparation

The formulation was prepared in two steps. Firstly NLC were produced by the emulsification-ultrasonication method [20]. Briefly, the mixture of lipids, with and without BVC in its base form (obtained from the hydrochloride species, as described before [21]) was melted in a water bath at 65 °C, above the melting point of the solid lipid (cetyl palmitate), and a solution of P68 was heated to the same temperature. Both phases were blended under high-speed agitation (10,000 rpm), for 3 min in an Ultra-Turrax blender (IKA WerkeStaufen, Germany). After, the mixture was sonicated for 30 min at 500 W and 20 kHz, in alternating 30 s (on and off) cycles, in a Vibracell tip sonicator (Sonic & Mat. Inc., Danbury, USA). The resultant nanoemulsion was immediately cooled to room temperature with an ice bath, to produce nanostructured lipid carriers with bupivacaine (NLC<sub>BVC</sub>) and a control formulation without the anesthetic (NLC<sub>FREE</sub>). In the second step, a solution of sodium alginate was prepared in deionized water, and the NLC formulation was added to it under agitation for 15 min, until the formation of a homogeneous liquid suspension. The hybrid formulation (Hybrid<sub>BVC</sub>) and its control, prepared without bupivacaine (Hybrid<sub>FREE</sub>) were stored at ambient temperature (25–30 °C) for further use. The concentration of each excipient in the formulations is given in Table S1.

### 2.3. Characterization of the formulation

#### 2.3.1. Particle size, polydispersity index, zeta potential

A Nano ZS90 analyzer (Malvern Instruments, UK) was used to determine the hydrodynamic size and polydispersity index (PDI) of the nanoparticles - by dynamic light scattering (DLS) - and their zeta potentials (ZP), by laser doppler microelectrophoresis [22]. All the analyzed samples were diluted in deionized water ( $n = 3$ ).

#### 2.3.2. Bupivacaine quantification and encapsulation efficiency (%EE) determination

A Varian ProStar high performance liquid chromatography (HPLC) equipment with a PS 325 UV-Vis detector, a PS 210 solvent delivery module and Galaxy Workstation software for data collection, was used for the quantification of BVC. The column used was a Gemini® 5 µm, C18, 110 Å (150 mm × 4.6 mm) (Phenomenex®, Torrance, USA) with a

mixture of 0.1% v/v phosphoric acid:acetonitrile (70:30 v/v) as the mobile phase, at a flow rate of 1 mL/min. The injection volume was 30 µL and the absorbance was followed in 210 nm [19]. The total amount of BVC (BVC<sub>total</sub>) in the formulations was determined by diluting the samples in the mobile phase ( $n = 3$ ) [19,23]. The encapsulation efficiency (%EE) was determined by the ultrafiltration-centrifugation method, using cellulose filters (30 kDa, Millipore). The initial concentration of BVC (BVC<sub>total</sub>) and that in the filtrate (BVC<sub>free</sub>) were measured, and %EE was calculated according to Eq. (1) [19,23]:

$$\%EE = \frac{BVC_{total} - BVC_{free}}{BVC_{total}} \times 100 \quad (1)$$

### 2.4. Structural analysis

#### 2.4.1. Transmission Electron Microscopy

Micrographs of the samples were obtained using a JEOL 1200 EXII microscope operated at 60 kV. For preparing the samples (1% (w/w) of alginate (ALG), NLC<sub>FREE</sub>, NLC<sub>BVC</sub>, Hybrid<sub>FREE</sub> and Hybrid<sub>BVC</sub>), uranyl acetate (2%) was added to the diluted samples (20×) to provide contrast. After, the aliquots were deposited onto copper grids coated with a carbon film and dried at room temperature.

#### 2.4.2. Differential scanning calorimetry (DSC) and X-Ray diffraction analysis (XRD)

DSC thermograms were collected in a 2910 TA calorimeter (TA Instruments, DE, USA) and analyzed with Thermal Solutions v.1.25 (TA Instruments, DE, USA) software. Cetyl palmitate, BVC base (excipients) and the freeze-dried samples of 1% ALG, 0.5% BVC in 1% ALG w/w (ALG + BVC), NLC<sub>FREE</sub>, NLC<sub>BVC</sub>, Hybrid<sub>FREE</sub> and Hybrid<sub>BVC</sub> were heated using a hermetic aluminium sample pan at the rate of 10 °C/min, with the temperature ranging from 20 to 150 °C.

To obtain the powder X-ray diffraction (XRD) data, a Shimadzu XRD7000 diffractometer (Tokyo, Japan), using a Cu-Kα source, was used. The same samples described above (DSC) were analyzed. Diffractograms were run at a scan step of 2°/min, between 2θ values (5 and 50°).

#### 2.4.3. Infrared analysis (ATR-FTIR)

The spectra of freeze-dried pure excipients (ALG, CP, P68, BVC), physical mixture (alginate + P68) and samples (ALG + BVC, NLC<sub>FREE</sub>, NLC<sub>BVC</sub>, Hybrid<sub>FREE</sub>, Hybrid<sub>BVC</sub>) were collected using an Agilent Cary 630 FTIR instrument equipped with ATR module. The data were collected between 4000 and 650 cm<sup>-1</sup>, with 4 cm<sup>-1</sup> of resolution.

### 2.5. Physicochemical stability

The physicochemical stability of the hybrid systems stored at room temperature (25–30 °C) was followed for 12 months. Nanoparticle size (nm), PDI and ZP (mV) were the measured parameters. Analysis of variance (one-way ANOVA, 95% confidence level) and Tukey *post hoc* test were employed to compare inter-groups significant differences, regarding the initial time measurements.

### 2.6. In vitro release experiment

The *in vitro* release of BVC (pKa = 8.1 [2]) was studied using a 12 mL Franz diffusion cell system, with 5 mM PBS buffer (pH 7.4) and 2.5 mM CaCl<sub>2</sub> as the receptor solution, separated from the acceptor chamber by a polycarbonate membrane (Nucleopore Track-Etch, 19 mm diameter, 0.1 µm pore size, Whatman®); the samples were kept at 37 °C under stirring at 300 rpm ( $n = 6$ ) [24]. The formulations tested (100 µL added in the donor chamber) were: 0.5% enantiomeric excess bupivacaine hydrochloride (BVC), ALG + BVC, NLC<sub>BVC</sub> and Hybrid<sub>BVC</sub>. At determined time intervals (0.15, 1, 2, 4, 6, 8, 22, 24, 28 h) samples of 200 µL were collected of the sampling port and replaced

with fresh receptor solution, not to surpass the solubility of BVC (0.57 mM according to [25]). The amount of BVC in the collected samples was quantified by HPLC. The KinetDS 3.0 software was used for the quantitative analysis of the total data of the obtained release curves [26]. Several kinetic models were tested (zero order, first order, Weibull, Higuchi, Hiscon-Crowell and Korsmeyer-Peppas) and, according to the  $R^2$  coefficient, the best fit for the hybrid formulation was obtained with the Weibull model (Eq. (2)):

$$m = 1 - \exp\left[\frac{-t^n}{a}\right] \quad (2)$$

where,  $m$  is the amount of BVC released as a function of time ( $t$ ), and  $a$  denotes a scale parameter that describes the time dependence of the release.

## 2.7. In vivo tests

### 2.7.1. Analgesic efficacy (paw withdrawal threshold test)

The experimental protocol for the *in vivo* tests was approved by the UNICAMP Institutional Animal Care and Use Committee (CEUA-UNICAMP protocol #4155-1), which follows the recommendations of the Guide for the Care and Use of Laboratory Animals. Briefly, adult male Wistar rats (*Rattus norvegicus albinus*, weighting 250–350 g) were randomly divided in batches of 5 animals with no restriction to water and food; the animals were previously acclimated for 15 days at the place of experimentation under 12 h light/dark cycles and controlled temperature and humidity. For the tests, 0.2 mL of each formulation was injected into the popliteal space, posterior to the knee joint, in the sciatic nerve area [27] in the right rat paws. An analgesimeter (Ugo Basile, Varese, Italy) was used to measure the sensory nerve block, by the paw pressure test [28]. The Paw Withdrawal Threshold to Pressure (PWTP) was determined taking into account the registered force (in grams) on the injected paw. The *cut-off* value was 180 g and baseline values of 30–50 g were selected as the pain threshold; animals with lower or higher values than the baseline were excluded. The first measurements were carried out 30 min and 1 h after injection. After that, the measurements were done in 1 h intervals, for 30 h. The obtained values were converted into maximum possible effect (% MPE) data, according to Eq. (3) [29]:

$$\%MPE = \frac{(\text{threshold} - \text{baseline})}{(\text{cutoff} - \text{baseline})} \quad (3)$$

where %MPE is the percentage of maximum possible effect, *threshold* corresponds to the measured pressure values, *baseline* is the standard value of each animal, and *cut-off* refers to the limit (180 g) pressure adopted, to avoid skin injury.

The area under the curve (AUC) of analgesic effect was calculated through the %MPE plot. Statistical analyses were performed by One-Way ANOVA with Tukey-Kramer post-test, using GraphPad Prism version 6.00 for Windows (California, USA).

### 2.7.2. In vivo imaging

For the *in vivo* imaging, NLC were labeled with the fluorescent dye DID (0.01% w/w,  $\sim 6 \times 10^{-4}$  mol%), added to the lipid phase [30]. Four-week-old male C57BL/6JUnib mice were kept in appropriate micro-isolators, under 12 h light-dark cycles, with controlled temperature and humidity, receiving water and food *ad libitum* (Committee for Ethics in Animal Use CEUA-UNICAMP protocol #4999-1). 50  $\mu$ L of the formulations (NLC<sub>FREE</sub> and Hybrid<sub>FREE</sub>) were injected in the right paw into the popliteal space, posterior to the knee joint, in the sciatic nerve area ( $n = 5$ ). After one hour of application, and after 1, 2, 3, 4, 7, 9, 11 and 14 days after injection, the animals were imaged using an *in vivo* imaging analyzer (*in vivo* FX-PRO, Bruker, TX, USA). For that, fluorophore excitation and emission wavelengths were set to 630 and 700 nm, respectively, and the imaging time was 1 min. Additionally, mice were X-rayed for the anatomical localization of the labeling.

**Table 1**

Physicochemical results of nanostructured lipid carriers - without and with bupivacaine (NLC<sub>FREE</sub> and NLC<sub>BVC</sub>, respectively) - and Hybrid formulations - without and with bupivacaine (Hybrid<sub>FREE</sub> and Hybrid<sub>BVC</sub>, respectively) - regarding size (nanometers, nm), polydispersity index (PDI), Zeta potential (mV) and encapsulating efficiency (%EE).

Formulation	Size (nm)	PDI	Zeta potential (mV)	%EE
NLC <sub>FREE</sub>	181.4 ± 1.4	0.130 ± 0.017	-29.8 ± 1.0	-
NLC <sub>BVC</sub>	185.6 ± 1.5	0.134 ± 0.006	-34.4 ± 0.3	54.5 ± 1.2
Hybrid <sub>FREE</sub>	196.8 ± 3.1	0.150 ± 0.014	-39.4 ± 0.8	-
Hybrid <sub>BVC</sub>	198.4 ± 1.5	0.170 ± 0.015	-44.2 ± 0.8	59.1 ± 2.0

During the imaging procedures, mice were kept under anesthesia (isoflurane 3%). The images and data of area and intensity were collected using the Molecular Imaging (Bruker, v. 7.1.3.20550) software, and the statistical analyses were done using GraphPad Prism version 6.00 for Windows (California, USA).

## 3. Results

In the development of hybrid DDS formulations, the possible interference of one carrier system over the other should be considered. Thus, Table 1 compares the nanoparticles size, polydispersity and surface charge in four samples: nanostructured lipid carriers without enantiomeric excess-bupivacaine (NLC<sub>FREE</sub>), nanoparticles with bupivacaine (NLC<sub>BVC</sub>) and nanoparticles in the hybrid systems (NLC plus alginate and without bupivacaine, Hybrid<sub>FREE</sub>) and nanoparticles plus alginate and bupivacaine (Hybrid<sub>BVC</sub>). The encapsulation efficiency of bupivacaine in the NLC<sub>BVC</sub> and Hybrid<sub>BVC</sub> formulations is also given.

### 3.1. Structural analyses

#### 3.1.1. Transmission electron microscopy

This technique is often used to obtain information about the morphology of the nanoparticles [31–33]. In Fig. 1A and B, we can see images of the alginate polymer mesh. Fig. 1C and D show the shape of control NLCs, spherical and regular, with defined borders. Addition of alginate (to form the hybrid system) did not change NLC's morphology, and the nanoparticles got inserted inside the polymer alginate mesh, as evidenced in Fig. 1E, F, G and H. In the same way, no differences in morphology were found between the formulations, with and without bupivacaine in enantiomeric excess (Fig. 1E, F vs. Fig. 1G, H).

#### 3.1.2. Differential scanning calorimetry (DSC) and X-ray diffraction analysis (XRD)

The combination of DSC and XDR is usually applied to study the crystalline structure of NLC [8] as well as to collect evidences of drug encapsulation [34,35]. Fig. 2A and Table S2 show the results of DSC analysis. For NLC<sub>FREE</sub>, where CP (transition temperature: 57.7 °C) and P68 (transition temperature: 54.5 °C) are excipients, just one thermal event was registered at 54.4 °C. When BVC is present (NLC<sub>BVC</sub>), there is a decrease in the transition temperature (to 54.1 °C) and enthalpy (from 221.9 to 106.3 J/g), relatively to NLC<sub>FREE</sub>. These data indicate that the fraction of BVC that gets encapsulated in the NLC (%EE = 54.5%, Table 1) decreases the crystallinity of the lipid core, as previously observed with other local anesthetics [35]. In relation to alginate, results are indicative of its association with the nanoparticles, since it induced an increase in the transition temperature of the nanoparticles (from 54.4 °C in NLC<sub>FREE</sub> to 57.2 °C in Hybrid<sub>FREE</sub>). The same increase in the transition temperature was observed (54.1 to 56.0 °C) in the presence of the anesthetic (NLC<sub>BVC</sub> vs. Hybrid<sub>BVC</sub>, Table S2). This result indicates that the presence of BVC does not influence the interaction of alginate with the NLC.

The results of X-ray diffraction (XRD) show that cetyl palmitate, the

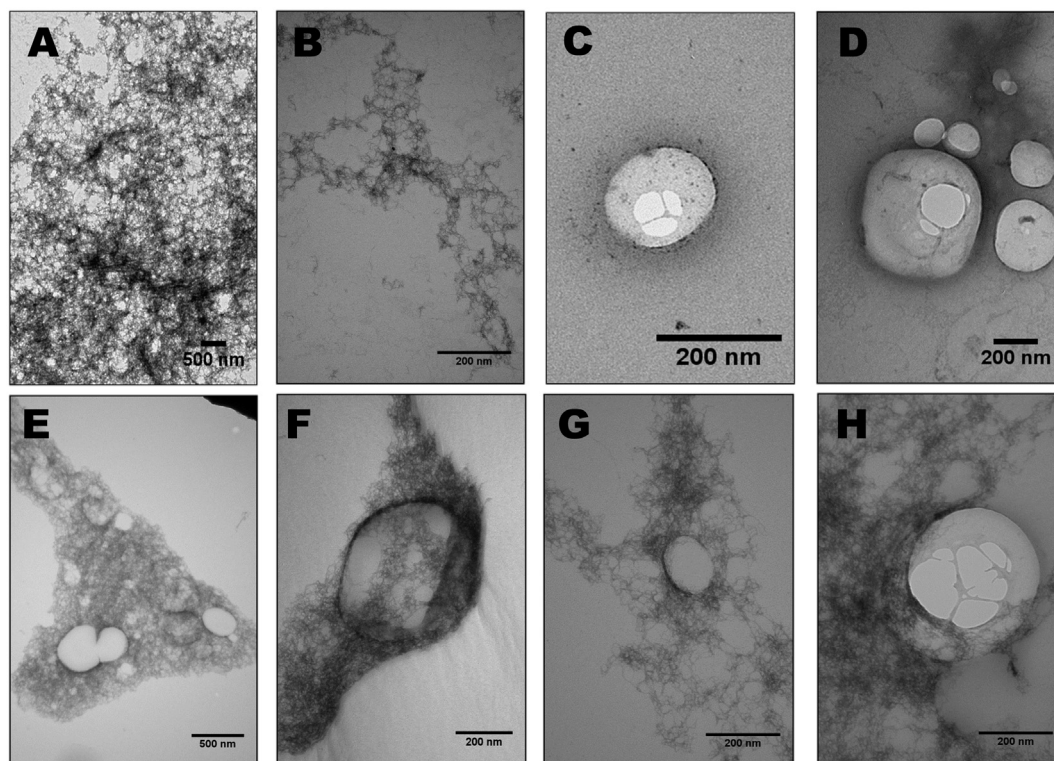


**Fig. 1.** TEM images of pure alginate (A, B), and nanostructured lipid carriers in samples:  $NLC_{FREE}$  (C, D),  $Hybrid_{FREE}$  (E, F) and  $Hybrid_{BVC}$  (G, H). Magnification:  $10000\times$  (A),  $35,970\times$  (E),  $60,000\times$  (B) and  $100,000\times$  (C, D, F, G, H).

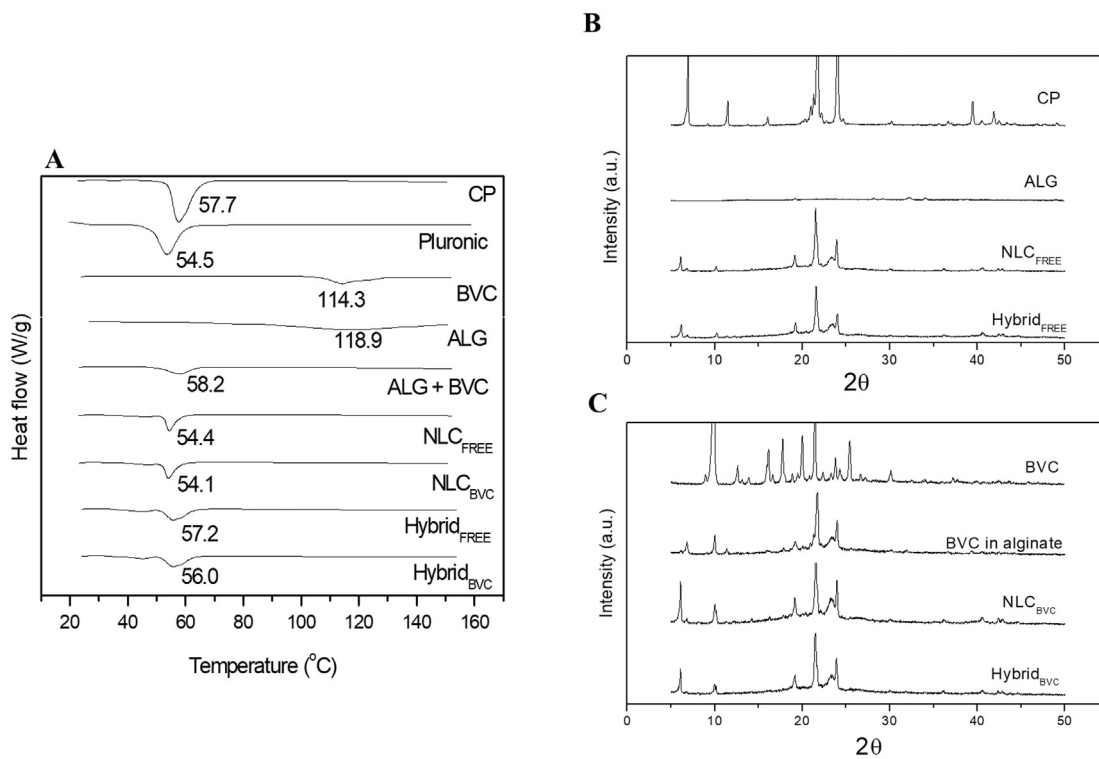


**Fig. 2.** A) DSC thermograms, obtained at a heating rate of  $10\text{ }^{\circ}\text{C}/\text{min}$ . B,C) X-ray diffractograms obtained with a Cu-K $\alpha$  source, at a scan step of  $2^{\circ}/\text{min}$ , graphed in the same scale, for: B) cetyl palmitate (CP), alginate (ALG), NLC and hybrid formulations without bupivacaine ( $NLC_{FREE}$  and  $Hybrid_{FREE}$ ); C), bupivacaine in enantiomeric excess (BVC), BVC in alginate (ALG + BVC), NLC and hybrid formulations with bupivacaine ( $NLC_{BVC}$  and  $Hybrid_{BVC}$ ).

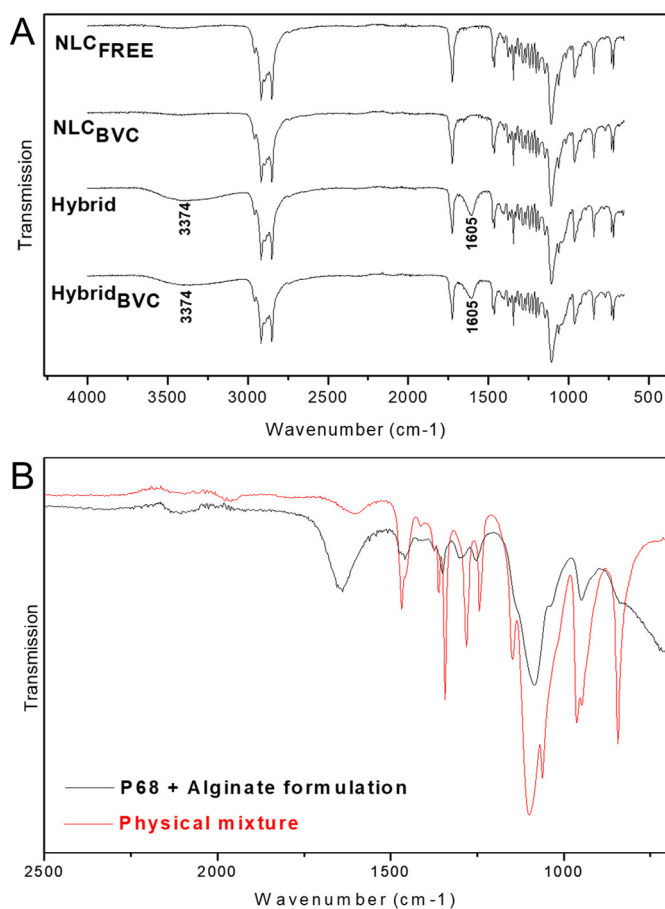


Fig. 3. FTIR-ATR spectra of: A) NLC and hybrid formulations; B) physical mixture and formulation of Pluronic F-68 and alginate (see text).

main lipid component and responsible for the solid core of the nanoparticles, shows intense peaks at 7, 11, 21 and 24°, indicating its crystalline structure (Fig. 2B) [35]. As expected, the intensity of these CP peaks decreased, both in NLC and hybrid formulations (Fig. 2B). However, there was no difference in the decrease of intensity relatively to pure CP, when the hybrid formulation is compared to the NLC, suggesting that alginate seems not to interfere with the organization of cetyl palmitate into the NLC core. Also the crystalline structure of BVC – mainly its main peak at 10° [36] – is affected in all formulations (Fig. 2C). Altogether DSC and XRD analyses endorsed the %EE data, showing that BVC is incorporated in the lipid core of NLC and interacts also with alginate.

### 3.1.3. Infrared analysis

Infrared analysis (FTIR-ATR) is another useful tool for the characterization of nanostructured lipid carriers [14], and alginate [37]. The spectra of the main components of the hybrid system (cetyl palmitate, Pluronic F68, alginate and BVC) are given in Fig. S1 (supplementary material). Fig. 3A shows the spectra of the studied formulations. The infrared spectra of NLC and hybrid formulations (Hybrid<sub>FREE</sub> and Hybrid<sub>BVC</sub>) show similarities to the spectrum of nanoparticles' major lipid component, cetyl palmitate [35]. We observed that the difference in the hybrid formulations is the appearance of bands in 3374 and 1605 cm<sup>-1</sup>, corresponding to  $\nu_{OH}$  (and OH) and  $\nu_{asCO}$  ( $-COO^-$ ) that are distinctive of pure alginate [38] (Fig. S1). All the remaining spectra seem to be unchanged, indicating that alginate does not interact with the lipid core of NLC, in agreement with results obtained in the previous analyzes (TEM and XRD).

Since Infrared spectrum is dominated by the lipid-core components, mainly CP, which apparently does not interact with alginate, we

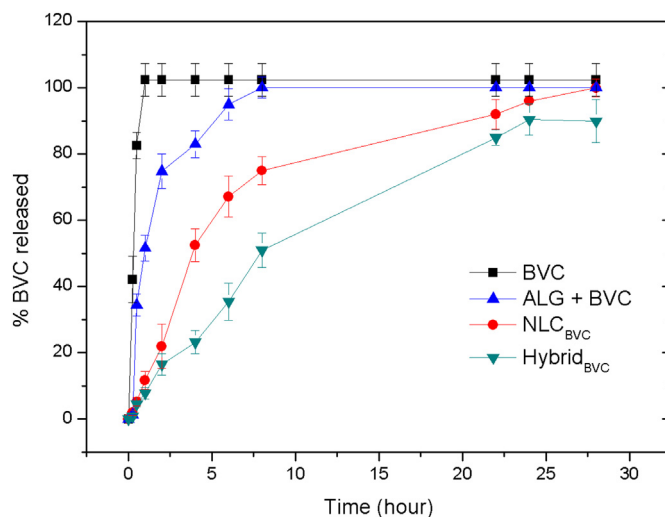


Fig. 4. *In vitro* release profiles of bupivacaine determined at 37 °C: in solution (BVC), in alginate solution (ALG + BVC), encapsulated in the nanostructured lipid carriers (NLC<sub>BVC</sub>), and in the hybrid formulation (Hybrid<sub>BVC</sub>). ( $n = 6$ ).

removed the lipid core from the nanoparticles aiming at detecting any interaction between the hydrophilic (polyethyleneglycol) chain of the P68 surfactant (Fig. S2) and alginate (Fig. S3). Thus, a formulation containing P68 and alginate, in the same concentrations used in the NLC and hybrid formulations, respectively, was prepared. Considering that at the concentration used (5% w/w), P68 in solution is in its micellar form [39], it is reasonable to expect that only its hydrophilic portion gets exposed, in order to interact with alginate (in a similar way to the orientation of P68 molecules in NLC). Also, a physical mixture (simple mixture of freeze-dried alginate and P68) was prepared for comparative reasons.

Fig. 3 shows the FTIR-ATR spectra of the physical mixture prepared with P68, after addition of alginate and subsequent freeze-drying. The spectrum of a formulation of the same composition is also given. Fig. 3B shows that the, in the formulation the characteristic band of alginate around 1600 cm<sup>-1</sup> is shifted towards higher wavenumbers in the presence of P68, in comparison to the physical mixture. Another information came from the disappearance of the band at 843 cm<sup>-1</sup> referring to CH stretching of the PPO chain of P68 (hydrophobic region, Fig. S2), confirming the micellar conformation [40] of the detergent in the formulation, but not in the physical mixture. Thus, FTIR-ATR results are indicative of interaction between the hydrophilic portion of the P68 molecules and alginate, on the surface of the NLC.

### 3.2. *In vitro* release experiment

The results of the *in vitro* release experiments are shown in Fig. 4. While free BVC was completely released after 1 h, the NLC<sub>BVC</sub> formulation extended the anesthetic release up to 28 h, with a burst phase in the initial hours, due to the unencapsulated BVC fraction (see Table 1). A control formulation, containing bupivacaine in alginate (ALG + BVC) showed fast initial release, and total equilibrium release in 7 h. As for the hybrid formulation, it exhibited the longest equilibrium profile (> 28 h) with no pronounced burst release in the first hours. At this point, aiming at showing the nanogel formation by the addition of  $Ca^{2+}$  in the donor solution, pictures from the Franz cell donor compartment were taken after the experiment (Fig. S4).

The release curves in Fig. 4 were analyzed with the KinectDS3 software [26], using different mathematical approaches (zero order, first order, Weibull, Higuchi, Hiscon-Crowell and Korsmeyer-Peppas) (Table S3). For the release of bupivacaine from the NLC, the Korsmeyer-Peppas model was the best-fit model, considering the  $R^2$  values [13]. As for the hybrid formulation, the best-fit model was the Weibull

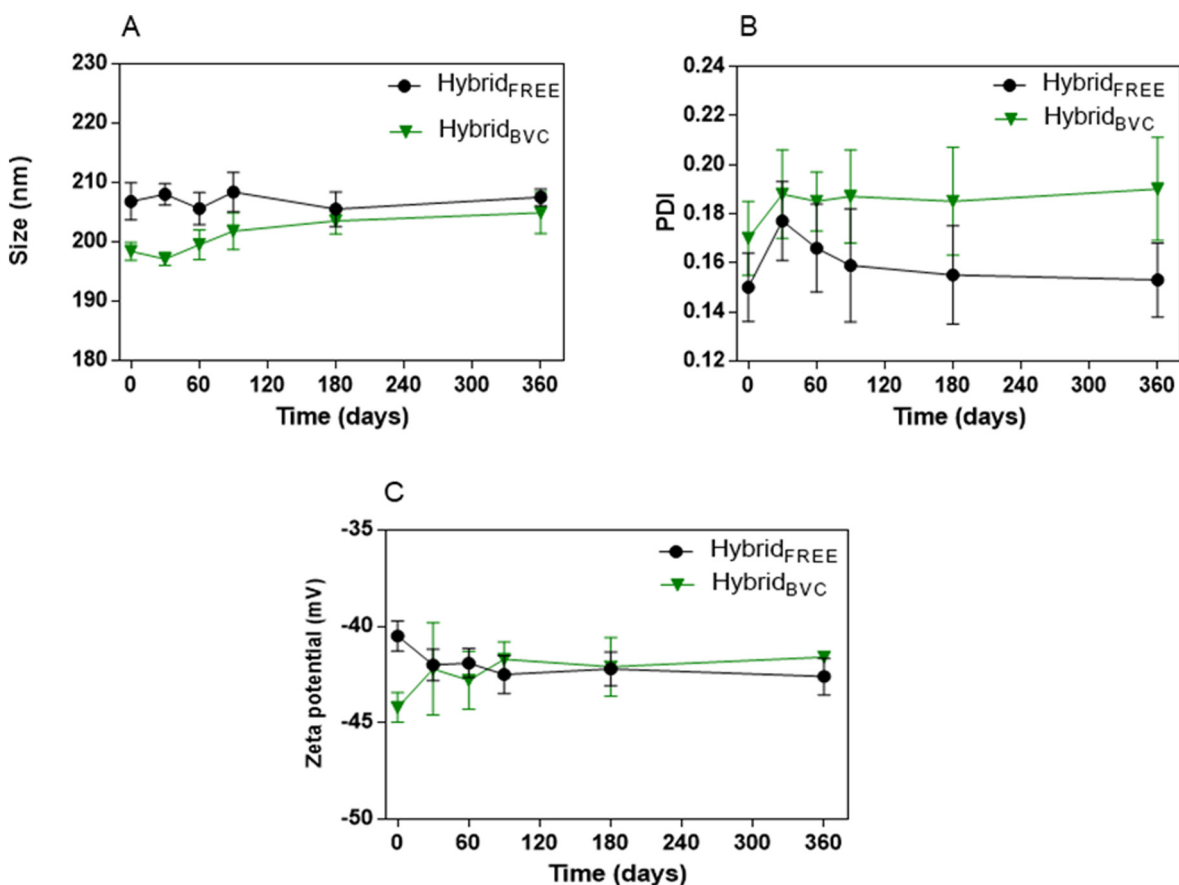


Fig. 5. Physicochemical stability of the hybrid formulation (Hybrid<sub>BVC</sub>) and its control (Hybrid<sub>FREE</sub>) considering size (A); PDI (B), and ZP (C) of the nanoparticles during 12 months of storage at room temperature. No statistically significant differences were observed (one-way ANOVA with Tukey *post hoc* test) in comparison to the initial results.

( $R^2 = 0.97$ ), in which the K parameter describes the shape of the curve (Eq. (2)). The determined value of K for the Hybrid<sub>BVC</sub> formulation ( $K = 1.49$ ) was higher than unit, indicating a sigmoidal release curve with a turning point [41]. Considering the other curves in Fig. 4 (NLC<sub>BVC</sub> and ALG + BVC), the slower release phase of the Hybrid<sub>BVC</sub> curve is probably explained by BVC release from the lipid NLC core into the alginate polymer, while the fast release regimen is due to BVC release from the alginate polymer.

### 3.3. Physicochemical stability

Alterations in the physicochemical features of NLC, such as polymorphic modifications in the lipid matrix [42–44], and any possible instability caused by addition of alginate are important to follow over the time. Thus, the physicochemical stability at room temperature of the Hybrid<sub>FREE</sub> and Hybrid<sub>BVC</sub> samples was followed for one year. The results are shown in Fig. 5 and Table S4. For the analyzed parameters (size, PDI, ZP), no statistically significant differences were observed, in comparison to the initial values.

### 3.4. In vivo tests

#### 3.4.1. Anesthetic efficacy

The anesthetic efficacy of the hybrid formulation was determined by the blockage of the rat sciatic nerve. With the paw withdrawal threshold test (PWPT), it was possible to quantify the duration and intensity of the sensory block induced by bupivacaine [45–47]. The maximum possible effect (MPE) found in formulations containing equivalent BVC (0.5%, clinical dose) concentration changed according to each formulation type and, as can be seen in Fig. 6A. BVC in solution

showed the shortest anesthetic duration (~4 h), followed by the ALG + BVC formulation (~7 h), NLC<sub>BVC</sub> (~10 h) and the Hybrid formulation (26–28 h). The curve in Fig. 6A shows that after achieving the maximum effect, the hybrid formulation sustained analgesia at the maximum for more than a day. Also, Hybrid<sub>BVC</sub> took longer to reach the maximum effect, a result predicted by the release test, where no burst release effect was observed. The hybrid formulation showed a prolonged anesthesia effect – ca. 650% higher than that of free BVC – as revealed by the area under the curve (AUC) data in Fig. 6B. To demonstrate the gel formation *in vivo*, control animals (those receiving formulations without bupivacaine) were euthanized shortly after (1 h) injection (Fig. 6C and D). In these animals, one can easily notice the nanogel formation near the region of anesthetic application, while the NLC formulation cannot be seen.

#### 3.4.2. In vivo imaging

*In vivo* imaging is a technique that has been gaining prominence in the development of nanoparticles because it opens the possibility of studying their properties in an organism without functional alterations [48]. Through the insertion of probes, it is possible to quantify, for instance, the fluorescence of the nanoparticulated systems, to follow their biodistribution and degradation [49]. Fig. 7 shows the results of the *in vivo* imaging experiments performed after the injection of NLC<sub>FREE</sub> and Hybrid<sub>FREE</sub> (labeled with DID fluorophore) in the sciatic nerve region of mice. Fig. 7A shows the decay of the fluorescence area in the same individual, after injection of the formulations. With the passage of the days, it is possible to see the decay of fluorescence area, confirming the degradation of the formulations in the organism. Looking at the NLC sample, at the fourth day of the experiment it was almost not possible to detect the nanoparticles in the injection region,

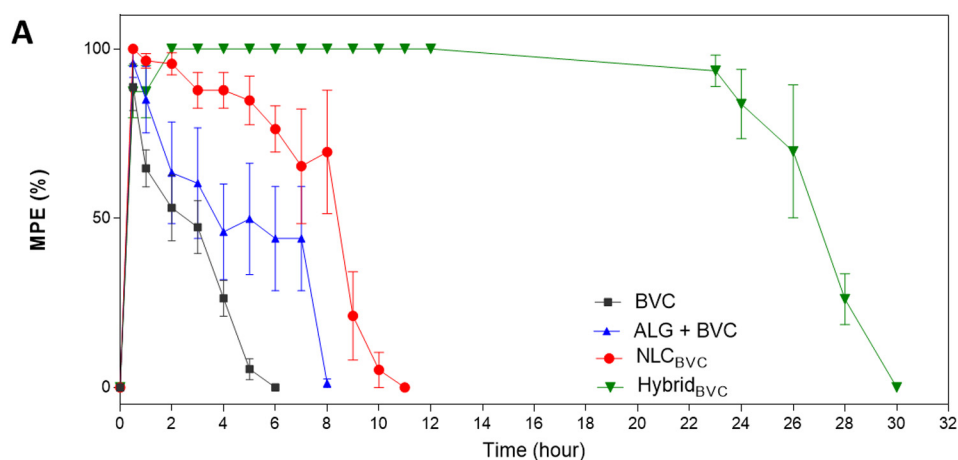


**Fig. 6.** Anesthetic efficacy measured through the PWPT test. (A) Maximum possible effect (MPE %) over time for formulations containing 0.5% bupivacaine: in solution (BVC), in alginate (ALG + BVC), encapsulated in nanostructured lipid carriers (NLC<sub>BVC</sub>) or in the hybrid formulation (Hybrid<sub>BVC</sub>), *n* = 5. (B) Area under the anesthesia curves (effect-time), according to A. C and D show images of euthanized control animals, after injection of nanostructured lipid carriers (left) and hybrid formulation without bupivacaine (right). Statistical tests: One-way ANOVA plus Tukey–Kramer *post hoc*: a, Hybrid<sub>BVC</sub> x BVC; b, Hybrid<sub>BVC</sub> x NLC<sub>BVC</sub>; c, Hybrid<sub>BVC</sub> x Alginate + BVC, d, NLC<sub>BVC</sub> x BVC. \* *p* < 0.05, \*\*\*\**p* < 0.0001.

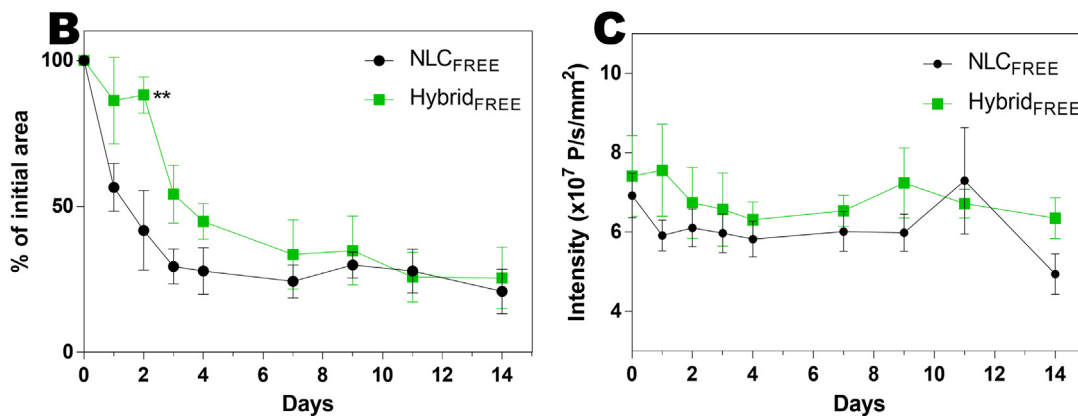
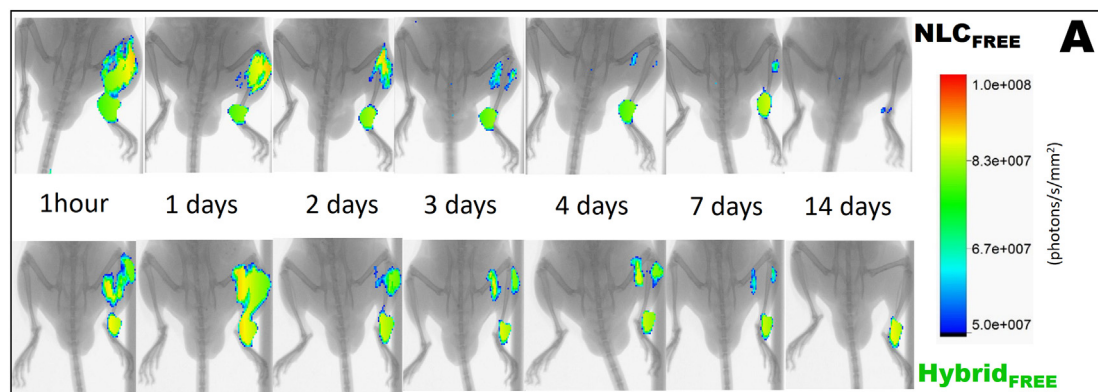
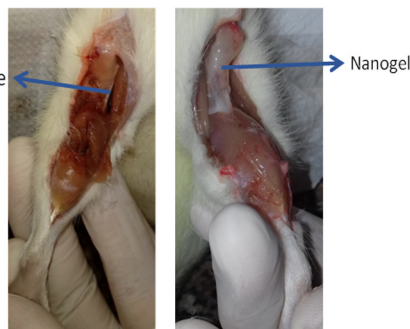
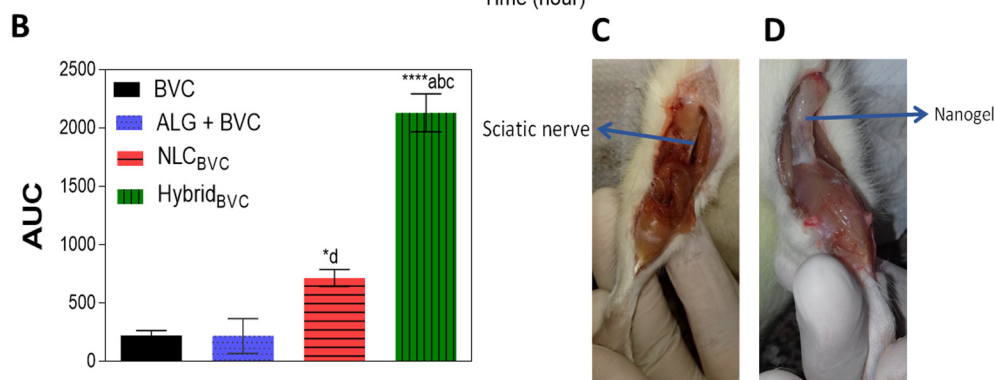


**Fig. 7.** *In vivo* imaging results. A, X-ray merged with fluorescent images of nanoparticles lipid carriers (NLC<sub>FREE</sub>) and the hybrid formulation (Hybrid<sub>FREE</sub>) in the different time points, in the same animal. B, changes in fluorescent area of the samples, in relation of initial area (%), mean and SEM) over the period. C, changes in intensity of fluorescent area (x10<sup>7</sup> photons/s/mm<sup>2</sup>, mean and SEM) over the time. Statistical tests: One-way ANOVA plus Tukey–Kramer *post hoc* in the same time point; \*\* *p* < 0.01. (*n* = 5).

posterior to the knee of the animal, while the fluorescent area in the hybrid formulation is still large. Furthermore, at the end of 14 days, while animals treated with the NLC<sub>FREE</sub> formulation showed almost no fluorescence, the hybrid formulation still elicited a fluorescence emission in the treated paw. This visual result is clearer after quantification (Fig. 7B and C). Fig. 7B shows the decay of the fluorescent area over time, showing that for the NLC formulation degradation starts one day after the application, whereas the hybrid formulation does not show any significant decrease in the first 2 days. Furthermore, Fig. 7C shows that detection of nanoparticles is higher in the hybrid formulation than in NLC formulation. This data corroborates the nanogel formation *in vivo* - the nanoparticles being more concentrated at the injection site, allowing a better detection in relation to the NLC formulation, which gets dispersed easily.

#### 4. Discussion

Drug delivery systems that provide safer administration of drugs, being easy to administer and containing biodegradable materials are highly desirable. In this work we combined two DDS carriers (NLC and alginate) which alone have good aptitudes for the encapsulation of local anesthetics, but that are not able to prolong anesthetic activity beyond a few hours [13,35,47,50]. The formulation joined the advantages of nanostructured particles that, dispersed in a polymeric matrix formed a new hybrid system that was effective in controlling pain for more than a day, using the regular clinical dose of enantiomeric excess bupivacaine (0.5%).

In relation to the structure of the developed system, the increase in size (~10 nm) and surface charge of the nanoparticles ( $\Delta ZP = 10$  mV, in modulus), as well as TEM images (Fig. 1G) show that NLC and alginate did form a new hybrid DDS. TEM images also revealed that NLC got distributed inside the alginate matrix, as expected for the interaction between the two carriers. Together, DSC and XRD evidenced a decrease in the crystalline structure inside NLC and Hybrid formulations, as well as after BVC encapsulation, in good agreement with the high %EE values in Table 1. Besides, XRD and FTIR-ATR data provided evidences that alginate did not interfere with the internal structure of the nanoparticles, while TEM analysis suggested an interaction between the NLC external components and alginate. According to FTIR-ATR spectra, when only the P68 surfactant (representing the exterior shell of the NLC) and alginate were analyzed, evidences from association between the two excipients were registered, from changes in the carbonyl groups of alginate and hydrophilic (PEO) groups of P68 (see structures in Figs. S2 and S3). Similar results were observed by Fan and colleagues [38] for the interaction between alginate and gelatin (that like P68, have hydroxyl groups in its structure) in blend fibers of these compounds, at different proportions.

*In vitro* release experiments are capable of identifying changes in the discharge of drugs from DDS, predicting their *in vivo* behavior. The pKa of BVC is 8.1 [2] so, in the buffer used, the concentrations used guarantee the sink condition. Besides, the *in vitro* formation of a nanogel was simulated: alginate gelation was induced by adding  $Ca^{2+}$  in the receptor compartment of Franz cells, to the same concentration of calcium in the serum [51]. As previously reported [13], the *in vitro* release profile of the anesthetic from NLC<sub>BVC</sub> followed the Korsmeyer-Peppas model. It indicated an anomalous non-Fickian transport for NLC<sub>BVC</sub>, where more than one mechanism rule BVC release: fast diffusion caused by the non-encapsulated drug fraction, and slow diffusion of the encapsulated anesthetic molecules. On the other hand, the sigmoidal release curve of the Hybrid<sub>BVC</sub> formulation was better described by the Weibull model. 3 phases of release were observed: the first - from time zero to 2.5 h - in which ca. 20% of BVC was fast liberated; the second - from 2.5 to 9 h - where ~ 55% of the anesthetic was discharged; and the third, with the slowest release rate, which last until the end of the experiment. Since gelification requires a drastic change in the molecular structure of alginate (that gets ionically crosslinked in an egg box

arrangement) we believe that such rearrangement restricted BVC diffusion, determining a more complex release profile. Indeed, in the hybrid system BVC displayed the most extended release, with a decrease in the initial burst release (Fig. 4) in comparison to NLC<sub>BVC</sub>. These results confirmed the prolonged release of Hybrid<sub>BVC</sub>, allowing us to predict its longer anesthetic time, confirmed after by the *in vivo* tests.

*In vivo* tests confirmed the distinguishing anesthetic effect achieved with the hybrid formulation, the formation of the nanogel *in vivo* (Fig. 6) and the reduction in nanoparticles degradation by the organism, favoring the drug release in the site of application for a longer time (Fig. 7). The goal of this formulation was to achieve greater modulation of bupivacaine release, at constant rates, effectively at the site of the action. Yet, using the usual clinical dose of bupivacaine (0.5%), the anesthesia duration could be improved by > 5 times. In addition, literature shows that 0.5% bupivacaine when incorporated in other DDS such as polymeric alginate nanoparticles [47] or multivesicular liposomes [52] promoted significantly shorter anesthesia times in sciatic nerve blockade, even in a gel formulation [53]. Equivalent anesthesia times (24 h) were reported only for racemic BVC in poly-lactide-co-glycolide microspheres, but at higher concentration (60% w/w) [54]. Therefore, the hybrid system described here achieved long lasting anesthesia with the clinical BVC dose, ensuring the systemic safety of its application.

The encapsulation of BVC in the lipid core of NLC (showed by %EE, DSC and XRD) and the interaction of NLC with alginate (DSC and FTIR data), with NLC surrounded by the polymeric alginate mesh (TEM), determined the complex release profile and prolonged *in vivo* analgesia time of the BVC hybrid formulation. As depicted in Fig. 8 for the Hybrid<sub>BVC</sub> formulation, we believe that the lipid core of the NLC serve as a reservoir in which bupivacaine was concentrated, while the alginate mesh involving the nanoparticles completes the modulation of the anesthetic release at the site of injection. The different release regimens in the release kinetics curves (Fig. 4) can be ascribed to at least two mechanisms: the fast release of BVC from the alginate polymer ( $k_1$  constant in Fig. 8), and the slower release of BVC from the lipid NLC core into the alginate polymer ( $k_2$  constant, Fig. 8), towards the medium. Thus, connecting the *in vitro* release data, the large increase in anesthesia time (PWPT test), and retention of the formulation at the site of action - measured by *in vivo* imaging, the hybrid system here described was found ideal for the delivery of local anesthetics. Moreover, other lipophilic drugs such as antitumor, antibiotics and anti-inflammatory could benefit from such binary drug delivery system, where a carrier serve as drug reservoir, and the other (gel) helps to regulate drug release. In addition, we foresee that to further increase the analgesia time, higher BVC doses can be tested, without impacting the systemic toxicity of the hybrid formulation, due to its ability to keep the anesthetic at the site of application.

#### 5. Conclusion

This work describes the development of a hybrid formulation by the coupling of a lipid carrier system (NLC) with a biopolymer (alginate). The hybrid system was physicochemically and structurally characterized, with evidences of interactions that explain its stability for a year. In physiological environment, where  $Ca^{2+}$  ions are present, gelification took place *in situ*, favoring the formulation to remain longer at the site of injection, increasing by > 5 times the duration of bupivacaine anesthesia, at its usual clinical dose (0.5%). Therefore, NLC formed a lipid reservoir of bupivacaine molecules - that was protected from clearance and metabolism - while alginate matrix modulated the release of the local anesthetic at the application site, in a very efficient delivery system, ideal for local anesthetics. This formulation is injectable (easy to apply), composed of safe and biodegradable excipients, do not require higher (toxic) BVC concentrations, being promising for the post-operative pain management to replace opioids and drugs of higher systemic effects.

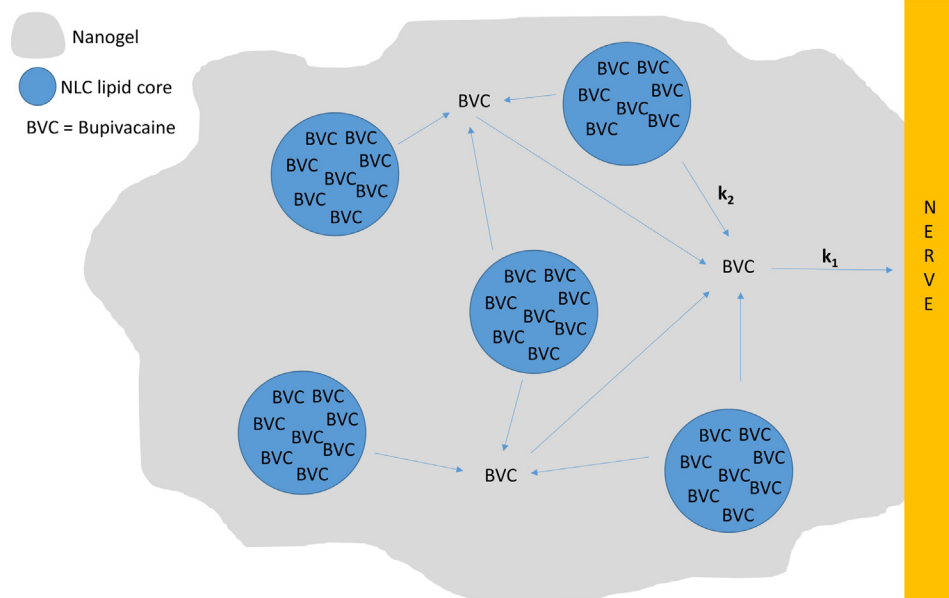


**Fig. 8.** Representative scheme of the hybrid formulation with a lipid core where the drug is concentrated, followed by release of the drug into the gel phase and then to the site of action (nerve).  $k_1$  denotes bupivacaine release from alginate to the medium, and  $k_2$  represents the release of bupivacaine from the NLC lipid core (see text).

### Author contribution statements

G.H.R.S.; G.G.; L.N.M.R.; V.G.; L.D.M.; A.L.B. and J.D.O. carried out the experiments. G.H.R.S. wrote the manuscript with the support of L.N.M.R.; M.C.B. and E.P. E.P. supervised the project and discussed/revised the manuscript. All authors discussed the results and commented on the manuscript.

### Declaration of competing interest

The authors declare they have no conflict of interest.

### Acknowledgments

The authors thank FAPESP (#14/14457-5) and INCT-Bioanalítica for research grants, and the fellowships from FAPESP (#17/15174-5, #14/25372-0, #18/07100-4 - G.H.R.S., L.N.M.R and G.G.), CAPES (L.D.M.) and CNPq (J.D.O, E.P.). We are also grateful to Cristália Prod. Quim. Farm. Ltda. for kindly providing Novabupi®; Dhaymer Ind. Com. Prod. Quim Ltda for the donation of cetyl palmitate; Gatefossé do Brasil for providing Capryol 90®, and Nervous Regeneration Laboratory / Unicamp for the *in vivo* imaging analyzer.

### Appendix A. Supplementary data

Supplementary data to this article can be found online at <https://doi.org/10.1016/j.msec.2019.110608>.

### References

- [1] A.P.H. Karlsen, M. Wetterslev, S.E. Hansen, M.S. Hansen, O. Mathiesen, J.B. Dahl, Postoperative pain treatment after total knee arthroplasty: a systematic review, *PLoS One* 12 (2017) e0173107, <https://doi.org/10.1371/journal.pone.0173107>.
- [2] D.R. de Araújo, L.N. de M. Ribeiro, E. de Paula, Lipid-based carriers for the delivery of local anesthetics, *Expert Opin. Drug Deliv.* 16 (2019) 701–714, <https://doi.org/10.1080/17425247.2019.1629415>.
- [3] E.C. Wick, M.C. Grant, C.L. Wu, Postoperative multimodal analgesia pain management with nonopioid analgesics and techniques, *JAMA Surg* 152 (2017) 691, <https://doi.org/10.1001/jamasurg.2017.0898>.
- [4] J. Shi, A.R. Votruba, O.C. Farokhzad, R. Langer, Nanotechnology in drug delivery and tissue engineering: from discovery to applications, *Nano Lett.* 10 (2010) 3223–3230, <https://doi.org/10.1021/nl102184c>.
- [5] R.H. Müller, D. Rühl, S.A. Runge, Biodegradation of solid lipid nanoparticles as a function of lipase incubation time, *Int. J. Pharm.* 144 (1996) 115–121, [https://doi.org/10.1016/S0378-5173\(96\)04731-X](https://doi.org/10.1016/S0378-5173(96)04731-X).
- [6] M.D. Joshi, R.H. Müller, Lipid nanoparticles for parenteral delivery of actives, *Eur. J. Pharm. Biopharm.* 71 (2009) 161–172, <https://doi.org/10.1016/j.ejpb.2008.09.003>.
- [7] L. Battaglia, M. Gallarate, Lipid nanoparticles: state of the art, new preparation methods and challenges in drug delivery, *Expert Opin. Drug Deliv.* 9 (2012) 497–508, <https://doi.org/10.1517/17425247.2012.673278>.
- [8] A. Gordillo-Galeano, C.E. Mora-Huertas, Solid lipid nanoparticles and nanostructured lipid carriers: a review emphasizing on particle structure and drug release, *Eur. J. Pharm. Biopharm.* 133 (2018) 285–308, <https://doi.org/10.1016/j.ejpb.2018.10.017>.
- [9] K.Y. Lee, D.J. Mooney, Alginate: properties and biomedical applications, *Prog. Polym. Sci.* 37 (2012) 106–126, <https://doi.org/10.1016/j.progpolymsci.2011.06.003>.
- [10] H.H. Tønnesen, J. Karlsen, Alginate in drug delivery systems, *Drug Dev. Ind. Pharm.* 28 (2002) 621–630, <https://doi.org/10.1081/DDC-120003853>.
- [11] L.N.M. Ribeiro, A.C.S. Alcântara, M. Darder, P. Aranda, P.S.P. Herrmann, F.M. Araújo-Moreira, M. García-Hernández, E. Ruiz-Hitzky, Bionanocomposites containing magnetic graphite as potential systems for drug delivery, *Int. J. Pharm.* 477 (2014) 553–563, <https://doi.org/10.1016/j.ijpharm.2014.10.033>.
- [12] L.N.M. Ribeiro, A.C.S. Alcântara, G.H. Rodrigues da Silva, M. Franz-Montan, S.V.G. Nista, S.R. Castro, V.M. Couto, V.A. Guilherme, E. de Paula, Advances in hybrid polymer-based materials for sustained drug release, *Int. J. Polym. Sci.* 2017 (2017) 1–16, <https://doi.org/10.1155/2017/1231464>.
- [13] G.H. Rodrigues da Silva, L.N.M. Ribeiro, H. Mitsutake, V.A. Guilherme, S.R. Castro, R.J. Poppi, M.C. Breikreitz, E. de Paula, Optimised NLC: a nanotechnological approach to improve the anaesthetic effect of bupivacaine, *Int. J. Pharm.* 529 (2017) 253–263, <https://doi.org/10.1016/j.ijpharm.2017.06.066>.
- [14] L.N.M. Ribeiro, M.C. Breikreitz, V.A. Guilherme, G.H.R. da Silva, V.M. Couto, S.R. Castro, B.O. de Paula, D. Machado, E. de Paula, Natural lipids-based NLC containing lidocaine: from pre-formulation to *in vivo* studies, *Eur. J. Pharm. Sci.* 106 (2017) 102–112, <https://doi.org/10.1016/j.ejps.2017.05.060>.
- [15] C. Puglia, M.G. Sarpietro, F. Bonina, F. Castelli, M. Zammataro, S. Chiechio, Development, characterization, and *in vitro* and *in vivo* evaluation of benzocaine- and lidocaine-loaded nanostructured lipid carriers, *J. Pharm. Sci.* 100 (2011) 1892–1899, <https://doi.org/10.1002/jps.22416>.
- [16] A. Hafezi, B. Amsden, Biodegradable injectable *in situ* forming drug delivery systems, *J. Control. Release* 80 (2002) 9–28, [https://doi.org/10.1016/S0168-3659\(02\)00008-1](https://doi.org/10.1016/S0168-3659(02)00008-1).
- [17] S. Cohen, E. Lobel, A. Trevigoda, Y. Peled, A novel *in situ*-forming ophthalmic drug delivery system from alginates undergoing gelation in the eye, *J. Control. Release* 44 (1997) 201–208, [https://doi.org/10.1016/S0168-3659\(96\)01523-4](https://doi.org/10.1016/S0168-3659(96)01523-4).
- [18] W. Zhang, W. Xu, C. Ning, M. Li, G. Zhao, W. Jiang, J. Ding, X. Chen, Long-acting hydrogel/microsphere composite sequentially releases dexmedetomidine and bupivacaine for prolonged synergistic analgesia, *Biomaterials* 181 (2018) 378–391, <https://doi.org/10.1016/j.biomaterials.2018.07.051>.
- [19] G.H.R. Da Silva, L.N. de Moraes Ribeiro, V.A. Guilherme, S.R. de Castro, M.C. Breikreitz, E. de Paula, Bupivacaine (S75:R25) loaded in nanostructured lipid carriers: factorial design, HPLC quantification method and physicochemical stability study, *Curr. Drug Deliv.* 15 (2017) 388–396, <https://doi.org/10.2174/1567201814666170726101113>.
- [20] C. Schwarz, W. Mehnert, J.S. Lucks, R.H. Müller, Solid lipid nanoparticles (SLN) for controlled drug delivery. I. Production, characterization and sterilization, *J. Control. Release* 30 (1994) 83–96, [https://doi.org/10.1016/0168-3659\(94\)90047-7](https://doi.org/10.1016/0168-3659(94)90047-7).
- [21] F. Cilirzo, F. Selmin, V. Liberti, L. Montanari, Thermal characterization of poly

- (lactide-co-glycolide) microspheres containing bupivacaine base polymorphs, *J. Therm. Anal. Calorim.* 79 (2005) 9–12, <https://doi.org/10.1007/s10973-004-0554-9>.
- [22] S. Bhattacharjee, DLS and zeta potential - what they are and what they are not? *J. Control. Release* 235 (2016) 337–351, <https://doi.org/10.1016/j.jconrel.2016.06.017>.
- [23] C.M. Moraes, E. de Paula, A.H. Rosa, L.F. Fraceto, Validation of analytical methodology by hplc for quantification of bupivacaine (s75-r25) in poli-lactide-co-glycolide nanospheres, *Quim Nova* 31 (2008) 2152–2155, <https://doi.org/10.1590/S0100-40422008000800040>.
- [24] W. Tiyaboonchai, W. Tungpradit, P. Plianbangchang, Formulation and characterization of curcuminoids loaded solid lipid nanoparticles, *Int. J. Pharm.* 337 (2007) 299–306, <https://doi.org/10.1016/j.ijpharm.2006.12.043>.
- [25] T.D. Wilson, Bupivacaine, *Anal. Profiles Drug Subst.* 1990, pp. 59–94, [https://doi.org/10.1016/S0099-5428\(08\)06364-0](https://doi.org/10.1016/S0099-5428(08)06364-0).
- [26] A. Mendoyk, R. Jachowicz, K. Fijorek, P. Doro, P. Kulinowski, S. Polak, P. Dorożyński, P. Kulinowski, S. Polak, KinetDS: an open source software for dissolution test data analysis, *Dissolution Technol. | Febr.* (2012) 6–11, <https://doi.org/10.14227/DT190112P6>.
- [27] N.F.S. de Melo, R. Grillo, V.A. Guilherme, D.R. de Araujo, E. de Paula, A.H. Rosa, L.F. Fraceto, Poly(Lactide-co-Glycolide) nanocapsules containing benzocaine: influence of the composition of the oily nucleus on physico-chemical properties and anesthetic activity, *Pharm. Res.* 28 (2011) 1984–1994, <https://doi.org/10.1007/s11095-011-0425-6>.
- [28] L.O. Randall, J.J. Selitto, A method for measurement of analgesic activity on inflamed tissue, *Arch. Int. Pharmacodyn. Thérapie.* CXI (1957) 409–419.
- [29] J.P. Penning, T.L. Yaksh, Interaction of intrathecal morphine with bupivacaine and lidocaine in the rat, *Anesthesiology* 77 (1992) 1186–2000 <http://www.ncbi.nlm.nih.gov/pubmed/1466469>, Accessed date: 2 January 2017.
- [30] R.R. Patlolla, M. Chougule, A.R. Patel, T. Jackson, P.N.V. Tata, M. Singh, Formulation, characterization and pulmonary deposition of nebulized celecoxib encapsulated nanostructured lipid carriers, *J. Control. Release* 144 (2010) 233–241, <https://doi.org/10.1016/j.jconrel.2010.02.006>.
- [31] F.-Q. Hu, S.-P. Jiang, Y.-Z. Du, H. Yuan, Y.-Q. Ye, S. Zeng, Preparation and characterization of stearic acid nanostructured lipid carriers by solvent diffusion method in an aqueous system, *Colloids Surfaces B Biointerfaces* 45 (2005) 167–173, <https://doi.org/10.1016/j.colsurfb.2005.08.005>.
- [32] A. Garg, K. Bhalala, D.S. Tomar, Wahajuddin, In-situ single pass intestinal permeability and pharmacokinetic study of developed Lumefantrine loaded solid lipid nanoparticles, *Int. J. Pharm.* 516 (2017) 120–130, <https://doi.org/10.1016/j.ijpharm.2016.10.064>.
- [33] B. Mohanty, D.K. Majumdar, S.K. Mishra, A.K. Panda, S. Patnaik, Development and characterization of itraconazole-loaded solid lipid nanoparticles for ocular delivery, *Pharm. Dev. Technol.* 20 (2015) 458–464, <https://doi.org/10.3109/10837450.2014.882935>.
- [34] S. Reis, N. Lúcio, L. Martins, Novel resveratrol nanodelivery systems based on lipid nanoparticles to enhance its oral bioavailability, *Int. J. Nanomedicine* 8 (2013) 177, <https://doi.org/10.2147/ijn.s37840>.
- [35] L.N.M. Ribeiro, M. Franz-Montan, M.C. Breikreitz, A.C.S. Alcântara, S.R. Castro, V.A. Guilherme, R.M. Barbosa, E. de Paula, Nanostructured lipid carriers as robust systems for topical lidocaine-prilocaine release in dentistry, *Eur. J. Pharm. Sci.* 93 (2016) 192–202, <https://doi.org/10.1016/j.ejps.2016.08.030>.
- [36] E.Y. Cheung, K.D.M. Harris, R.L. Johnston, S.J. Kitchen, K.L. Hadden, M. Zakrzewski, Rationalizing the structural properties of bupivacaine base—a local anesthetic—directly from powder X-ray diffraction data, *J. Pharm. Sci.* 93 (2004) 667–674, <https://doi.org/10.1002/jps.10551>.
- [37] E. Gómez-Ordóñez, P. Rupérez, FTIR-ATR spectroscopy as a tool for polysaccharide identification in edible brown and red seaweeds, *Food Hydrocol.* 25 (2011) 1514–1520, <https://doi.org/10.1016/J.FOODHYD.2011.02.009>.
- [38] L. Fan, Y. Du, R. Huang, Q. Wang, X. Wang, L. Zhang, Preparation and characterization of alginate/gelatin blend fibers, *J. Appl. Polym. Sci.* 96 (2005) 1625–1629, <https://doi.org/10.1002/app.21610>.
- [39] V.D. Samith, G. Miño, E. Ramos-Moore, N. Arancibia-Miranda, Effects of pluronic F68 micellization on the viability of neuronal cells in culture, *J. Appl. Polym. Sci.* 130 (2013) 2159–2164, <https://doi.org/10.1002/app.39426>.
- [40] Y.L. Su, J. Wang, H.Z. Liu, FTIR spectroscopic study on effects of temperature and polymer composition on the structural properties of PEO-PPO-PEO block copolymer micelles, *Langmuir* 18 (2002) 5370–5374, <https://doi.org/10.1021/la020007p>.
- [41] A.A. Cohen, Kant's biological conception of history, *J. Philos. Hist.* 2 (2008) 1–28, <https://doi.org/10.1163/187226308X268845>.
- [42] E. Souto, S. Wissing, C. Barbosa, R. Müller, Development of a controlled release formulation based on SLN and NLC for topical clotrimazole delivery, *Int. J. Pharm.* 278 (2004) 71–77, <https://doi.org/10.1016/j.ijpharm.2004.02.032>.
- [43] E. Gonzalez-Mira, M.A. Egea, E.B. Souto, A.C. Calpena, M.L. García, Optimizing flurbiprofen-loaded NLC by central composite factorial design for ocular delivery, *Nanotechnology* 22 (2011) 045101, <https://doi.org/10.1088/0957-4484/22/4/045101>.
- [44] K. Vivek, H. Reddy, R.S.R. Murthy, Investigations of the effect of the lipid matrix on drug entrapment, in vitro release, and physical stability of olanzapine-loaded solid lipid nanoparticles, *AAPS PharmSciTech* 8 (2007) 16–24, <https://doi.org/10.1208/p10804083>.
- [45] K. Leszczynska, S.T. Kau, A sciatic nerve blockade method to differentiate drug-induced local anesthesia from neuromuscular blockade in mice, *J. Pharmacol. Toxicol. Methods* 27 (1992) 85–93, [https://doi.org/10.1016/1056-8719\(92\)90026-V](https://doi.org/10.1016/1056-8719(92)90026-V).
- [46] D.R. de Araújo, L.F. Fraceto, A. de F. de A. Braga, E. de Paula, Drug-delivery systems for racemic bupivacaine (S50-R50) and bupivacaine enantiomeric mixture (S75-R25): cyclodextrins complexation effects on sciatic nerve blockade in mice, *Rev. Bras. Anesthesiol.* 55 (2005) 316–328, <https://doi.org/10.1590/S0034-70942005000300008>.
- [47] R. Grillo, N.F.S. de Melo, D.R. de Araújo, E. de Paula, A.H. Rosa, L.F. Fraceto, Polymeric alginate nanoparticles containing the local anesthetic bupivacaine, *J. Drug Target.* 18 (2010) 688–699, <https://doi.org/10.3109/10611861003649738>.
- [48] J.-L. Bridot, A.-C. Faure, S. Laurent, C. Rivière, C. Billotey, B. Hiba, M. Janier, V. Josseland, J.-L. Coll, L. Vander Elst, R. Muller, S. Roux, P. Perriat, O. Tillement, Hybrid gadolinium oxide nanoparticles: multimodal contrast agents for in vivo imaging, *J. Am. Chem. Soc.* 129 (2007) 5076–5084, <https://doi.org/10.1021/ja068356j>.
- [49] S. Ghiani, M. Capozza, C. Cabella, A. Coppo, L. Miragoli, C. Brioschi, R. Bonafè, A. Maiocchi, In vivo tumor targeting and biodistribution evaluation of paramagnetic solid lipid nanoparticles for magnetic resonance imaging, *Nanomedicine Nanotechnology, Biol. Med.* 13 (2017) 693–700, <https://doi.org/10.1016/J.NANO.2016.09.012>.
- [50] N.F.S. de Melo, E.V.R. Campos, C.M. Gonçalves, E. de Paula, T. Pasquoto, R. de Lima, A.H. Rosa, L.F. Fraceto, Development of hydrophilic nanocarriers for the charged form of the local anesthetic articaine, *Colloids Surfaces B Biointerfaces* 121 (2014) 66–73, <https://doi.org/10.1016/j.colsurfb.2014.05.035>.
- [51] T.M. Devlin, *Textbook of Biochemistry with Clinical Correlations*, Wiley, 2006, <https://doi.org/10.1017/CBO9781107415324.004>.
- [52] J.B. McAlvin, R.F. Padera, S.A. Shankarappa, G. Reznor, A.H. Kwon, H.H. Chiang, J. Yang, D.S. Kohane, Multivesicular liposomal bupivacaine at the sciatic nerve, *Biomaterials* 35 (2014) 4557–4564, <https://doi.org/10.1016/j.biomaterials.2014.02.015>.
- [53] X. Jia, G. Colombo, R. Padera, R. Langer, D.S. Kohane, Prolongation of sciatic nerve blockade by in situ cross-linked hyaluronic acid, *Biomaterials* 25 (2004) 4797–4804, <https://doi.org/10.1016/j.biomaterials.2003.12.012>.
- [54] R. Ohri, P. Blaskovich, J.C. Wang, L. Pham, G. Nichols, W. Hildebrand, D. Costa, N. Scarborough, C. Herman, G. Strichartz, Prolonged nerve block by micro-encapsulated bupivacaine prevents acute postoperative pain in rats, *Reg. Anesth. Pain Med.* 37 (2012) 607–615, <https://doi.org/10.1097/AAP.0b013e3182680f35>.